26th ABCM International Congress of Mechanical Engineering
November 22-26, 2021. Florianópolis, SC, Brazil

COB-2021-0732
STUDY OF THE INFLUENCE OF THE ZrO_2-$3Y_2O_3$ CONTENT ON THE Al_2O_3 MATRIX

Ana Carolina Agrizzi Araujo
Thales Vicente Mantovani Simões
Luma Gonçalves Fraga
Patrícia Alves Barbosa
Marcelo Bertolete Carneiro
Federal University of Espírito Santo, Department of Mechanical Engineering, 29075-910, Vitória/ES, Brazil
anacarolinaagrizzi@gmail.com, t_ha_mantovani@hotmail.com, luma.fraga@outlook.com, patricia.a.barbosa@ufes.br, marcelo.b.carneiro@ufes.br

Izabel Fernanda Machado
*University of São Paulo, Polytechnic School, Department of Mechatronics Engineering and Mechanical Systems, 05508-900, São Paulo/SP, Brazil
machadoi@usp.br

Francisco Guilhermo Briones Castilho*
Pontificia Universidad Católica de Valparaíso, Department of Mechanical Engineering, #2950, Valparaíso, Chile
francisco.briones@usp.br

Abstract. *Alumina-based ceramics have great relevance as cutting tool materials in the machining process of mainly ferrous materials, owing to their greater hardness retention, compressive strength, and chemical stability at elevated temperatures. The addition of ZrO_2 stabilized with Y_2O_3 in the Al_2O_3 matrix promotes phase transformation toughening and forms a composite known as zirconia-toughened alumina (ZTA). The aim of the work is to study the influence of the ZrO_2-$3Y_2O_3$ content (nanopowder) in the Al_2O_3 matrix (ultrafine powder) using the modern technique of pulsed electric current sintering (PECS) for the samples processing. The ZrO_2-$3Y_2O_3$ content was changed from 5 to 35% in volume. The powders were sintered at uniaxial pressure of 50 MPa and temperature of 1400ºC. Relative density, Vickers hardness, fracture toughness (K_{IC}) tests were performed and compared with commercial ceramic used as a reference. The results showed, for commercial ceramic, relative density of 98.2±0.3%, Vickers hardness number of 1712±306 HV, and K_{IC} equal to 4.22±0.67 MPa.m$^{1/2}$. For the sintered samples by PECS, the ZrO_2-$3Y_2O_3$ content aided to reach a full densification from 15%. All samples had Vickers hardness number greater than the reference. Although, the 5% ZrO_2-$3Y_2O_3$ sample had around 8% in porosity, it had the highest Vickers hardness number 2007±35 HV and K_{IC} 5.54±0.42 MPa.m$^{1/2}$. This analysis was important to highlight the properties for tailoring a functionally graded ceramic to be applied as a cutting tool.*

Keywords: *alumina, zirconia, density, Vickers hardness, fracture toughness*

1. INTRODUCTION

Alumina (Al_2O_3) is an engineering ceramic material used in structural applications, biomedical and aerospace areas (Basha and Sarkar, 2020). As structural application, in machining, in which environmental conditions are severe, ceramic cutting tools have abrasion resistance, high hot hardness, in addition to their chemical stability, which reduces the tendency to adhere to the workpiece materials during machining (Kalpakjian and Schmid, 2009). However, ceramics application working under mechanical loads and thermal shock conditions is limited due to their brittleness (Smuk, Szutkowska and Walter, 2003). Failure under such service conditions is usually related to the low fracture toughness value (Casellas *et al.*, 2003).

One of the methods to increase the fracture toughness is the addition of stabilized zirconia, ZrO_2, to the Al_2O_3 matrix, ceramic composites known as zirconia toughened alumina (ZTA). Zirconia has high strength and fracture toughness with good wear resistance (Kern *et al.*, 2015). Alumina and zirconia composites show improved fracture toughness owing to the toughening effect due to the phase transformation of stabilized zirconia, in which the tetragonal phase changes to the monoclinic phase with volume expansion, which can interrupt the crack propagation (Basha and Sarkar, 2020). Doping ZrO_2 with CaO, MgO, CeO_2 or Y_2O_3 ensures metastable phase of tetragonal ZrO_2 at room temperature, aiding strength and fracture toughness (Boniecki *et al.*, 2017).

Sintering is a process in which a group of loose or compacted particles are metallurgically bonded, forming a solid structure, improving strength and decreasing system energy. It occurs at high temperatures but below the melting point of the main constituent (German, 1998). Pulsed Electric Current Sintering (PECS) is a technique that combines pulsed electrical energy and mechanical pressure to promote the transformation of a powder, housed in a graphite mold, into a solid form with the desired composition and density (Zhou *et al.*, 2004). This technique promotes fast sintering, high thermal efficiency and uniform heating, being considered for sintering advanced materials, such as Functionally Graded Materials, FGM (Tokita, 2000).

FGM presents a special variation in composition and microstructure (Gong *et al.*, 2018). They provide a gradual transition of the properties of different materials from one side to the other, reducing the mismatch of properties of these materials to a minimum (Ma and Tan, 2001). This type of material is found in nature in bones and bamboo stems (Miyamoto *et al.*, 1999), in dental implants (Watari *et al.*, 1997), joint prostheses (Mishina, Inamaru and Kaitoku, 2008), ceramic tools self-lubricating (Xu *et al.*, 2014) and in experimental machining cutting tool (Bertolete *et al.*, 2020).

The objective of this work is to study the influence of the ZrO_2-$3Y_2O_3$ (nanopowder) content in Al_2O_3 matrix (ultrafine powder). Samples were processed by PECS. Density and mechanical properties were evaluated and compared with a commercial ceramic cutting tool. The results are intended to support the future development towards a functionally graded ceramic.

2. METHODOLOGY

2.1 Materials and powder preparation

Ultrafine α-Al_2O_3 (99.99% purity) powders and nanopowders ZrO_2-$3Y_2O_3$ (99.50%) provided by NanoAmor were used to produce samples. Results of density and mechanical properties of these samples were compared with those of a commercial ceramic cutting tool, CC620 (Sandvik). Table 1 lists some characteristics of the powders.

Table 1. Powders Characteristics

Material	Average particle size [µm]	Density [g/cm^3]	Modulus of elasticity [GPa]
α-Al_2O_3	0.20	3.97	380
ZrO_2-$3Y_2O_3$	0.04	5.90	210

Four samples with different powder volume fractions were defined. The concentration of ZrO_2-$3Y_2O_3$ (zirconia) was varied in α-Al_2O_3 (alumina) matrix, in proportions of 5, 15, 25 and 35%, see Table 2. The masses were measured and separated using a precision scale, model AD200 (Marte) with 0.001 g resolution. Each volume fraction was placed in different polypropylene bottles (65 ml). The mixture of powders was performed in a liquid environment of isopropyl alcohol for 30 hours, in a Wagner type mixer (New Lab), using grinding elements made of austenitic stainless steel in a mass ratio of 2:1 in relation to the powder. Then, they were dried in a laboratory drying oven model NL80/42 (New Lab) and deagglomerated in the mixer for 6 hours.

Table 2. Volumetric fraction of constituents for each sample.

Volume fraction of ZrO_2 [%]	Volume fraction of Al_2O_3 [%]
5	95
15	85
25	75
35	65

2.2 Sintering

The samples were sintered in a modern machine by pulsed electric current sintering (PECS), model 1050 (SPS Syntex Inc.). The machine has an automatic cycle control of current, voltage, temperature, pressure (P), atmosphere, as well as displacement.

A constant volume of powder, 1.8 g/cm^3, was manually placed into a cylindrical graphite mold (50 x 50 mm) grade MBIS60X (Morganite), see Figure 1 (a). To avoid adhesion among powders, mold walls and punches, a graphite sheet Grafoil GBT (Morganite) was used, also facilitating the removal of the sintered samples. The mold was placed between

punches-electrodes of a PECS machine, see Figure 1 (b), which promotes mechanical loading and electrical discharge, simultaneously. The sintered samples had a square-shaped geometry of 15 mm on the side with rounded corners.

A uniaxial pressure of 50 MPa and a vacuum atmosphere of ~10 Pa was applied to the powders. The heating rates from room temperature to 650°C and from 650°C to 1400°C were 104°C/min and 94°C/min. The dwell time at a temperature of 1400°C was 7 min. A 12 On 2 Off electrical current pulse pattern was used with 3.3 ms of pulse duration. Temperature was measured with a pyrometer directed to the side of the graphite mold surface. Sintering parameters were kept constant.

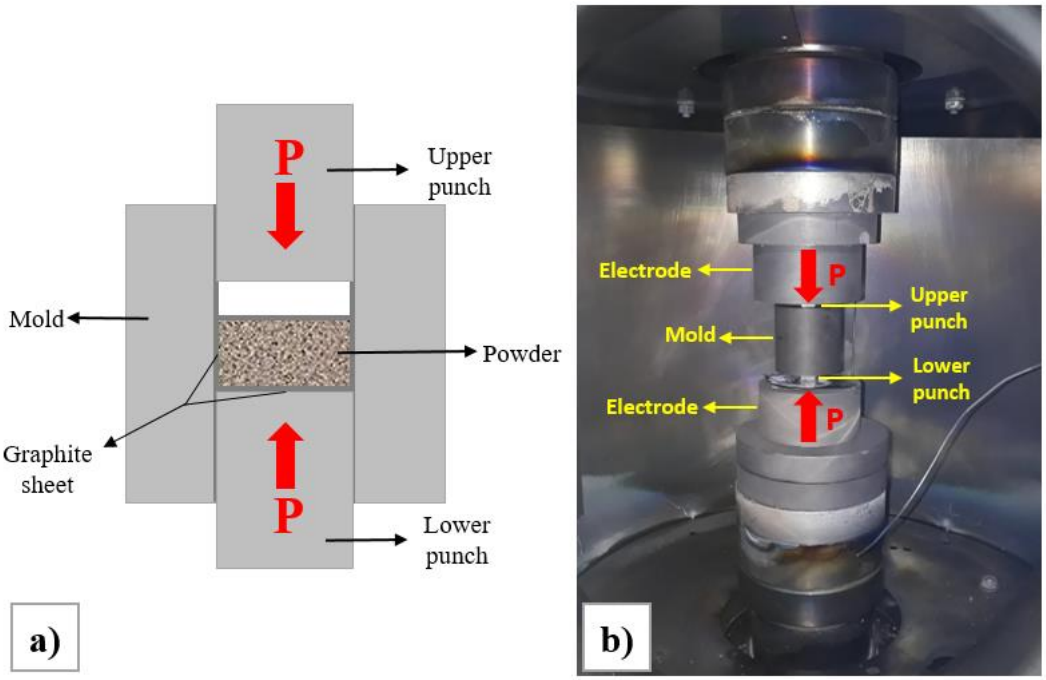

Figure 1. (a) Graphite mold assembly and (b) mold positioned inside the PECS machine.

2.3 Metallographic Preparation and Density Evaluation

The sintered samples were sectioned in half on a Minitom metallographic cutter (Struers), using a 15HC diamond disc (Buehler). One of the parts was mounted in a manual compression mounting machine model EFD 30 (FORTEL) with phenolic resin (bakelite) to carry out the Vickers hardness test and fracture toughness in cross section. The mounted samples had the apparent surface ground using SiC powder in grit sizes of #400, #600 and #1000, after polished with a diamond paste with particle size of 15 µm, 6 µm and 1 µm. Both steps were performed in a table-top unit PLFDV (FORTEL). Micrographic images were performed in scanning electron microscope (SEM), Stereoscan S440 (LEO).

The other half part was reserved for density evaluation. Relative density was measured following the ISO 10545-3 (1997) standard, which is based on the Archimedes Principle. A precision scale AD200 (Marte) with hydrostatic kit was used.

2.4 Mechanical Properties

The Vickers Hardness test was performed using the Universal Wolpert durometer. The Eclipse MA200 microscope (Nikon) was used to visualize and measure the indentations in the samples, as well as the cracks generated, see Figure 2. The test was carried out following the ASTM C1327-15 (2008) standard, using a load of 10 kgf and computing values from 10 acceptable indentations. The calculation of fracture toughness (K_{IC}) was performed by relating the Vickers hardness, modulus of elasticity, load and average length of cracks, Eq. (1).

$$K_{IC} = 0.016 \left(\frac{E}{H}\right)^{1/2} \frac{P}{c^{3/2}} \tag{1}$$

Where **E** is the modulus of elasticity [GPa] obtained from Eq. (2) (German and Park, 2008), **H** is the hardness value [GPa], **P** is the applied load [N], **c** the average length of the cracks measured from the center of indentation [m] and $\mathbf{K_{IC}}$ is given by [MPa.m$^{1/2}$]..

$$E = E_{alumina}V_{alumina} + E_{ZrO_2}V_{ZrO_2} \quad (2)$$

Where $\boldsymbol{E_{alumina}}$ and $\boldsymbol{E_{ZrO_2}}$ are the modulus of elasticity of alumina and zirconia, respectively.

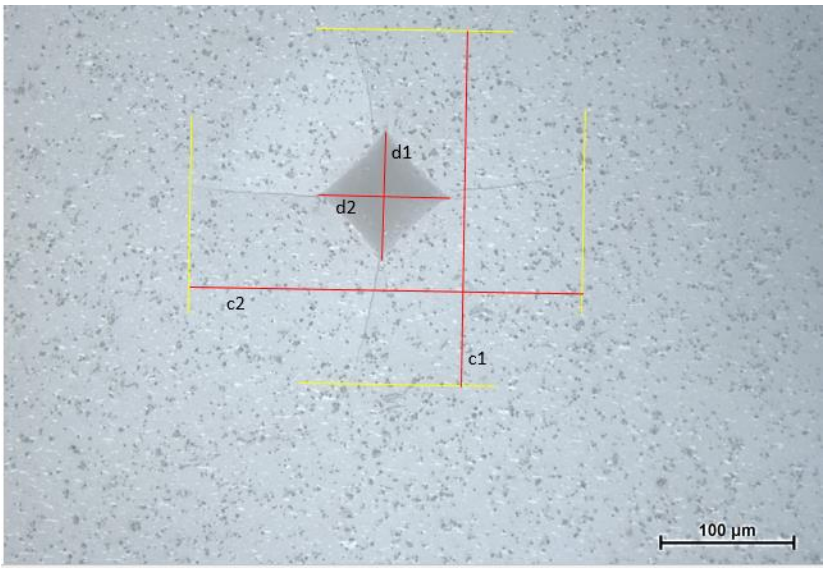

Figure 2. Illustration of the indentation performed on the Al_2O_3 sample with 15% ZrO_2 to assess the Vickers hardness and fracture toughness, where d1 and d2 are the diagonals of the indentation and c1 and c2 are the crack lengths.

It is worth mentioning that the cracking from the indentation tips did not interfere with the determination of tip location and thus the diagonal length measurements. According to the ASTM C1327-15 (2008) standard, the indentations are considered acceptable.

3. RESULTS AND DISCUSSION

3.1 Sintering

The sintering process monitoring was carried out for 34 minutes, see Figure 3. In the beginning, there is pressure application on the graphite punches that causes a mechanical displacement, initial point contact among particles. The initial sintering stage usually occurs during heating and is characterized by early stage neck growth. From 1100 ºC, around the 14th minute, a large shrinkage is observed; here porosity being consumed by interparticle neck growth, grain growth and pore shrinkage should be observed. This increase may have been intensified by the zirconia phase transformation, around 1170ºC, from the monoclinic to the tetragonal phase, presenting a reduction in its volume (Casellas *et al*., 2003; Boniecki *et al.*, 2017). During the dwell time at a temperature of 1400ºC, the pores reduce in size and grain growth occurs, the latter being a possible factor for a slight swelling of approximately 0.065 mm at the end of this period. From the beginning of the cooling, maintaining the work pressure, the sample presents further shrinkage, and when the pressure is relieved, a swelling.

3.2 Microstructure

The microstructure resulting from the sintering is dependent on the powder composition (German, 1996). Figure 4 shows the scanning electron microscopy (SEM) images of the sintered samples. Fine zirconia particles (white regions) are evenly distributed throughout the alumina matrix (grey region) in all samples, indicating that the mixing step provides homogeneous powder. In Figure 4 (a), it is possible to observe porosity (black dots) dispersed throughout the sample. As the ZrO_2 content is increased, the porosity is reduced, as can be seen in the sequence of Figure 4 (b), (c) and (d).The use of graphite sheets in the mold caused a certain amount of carbon to migrate into the sample, resulting in a darker coloration in the region.

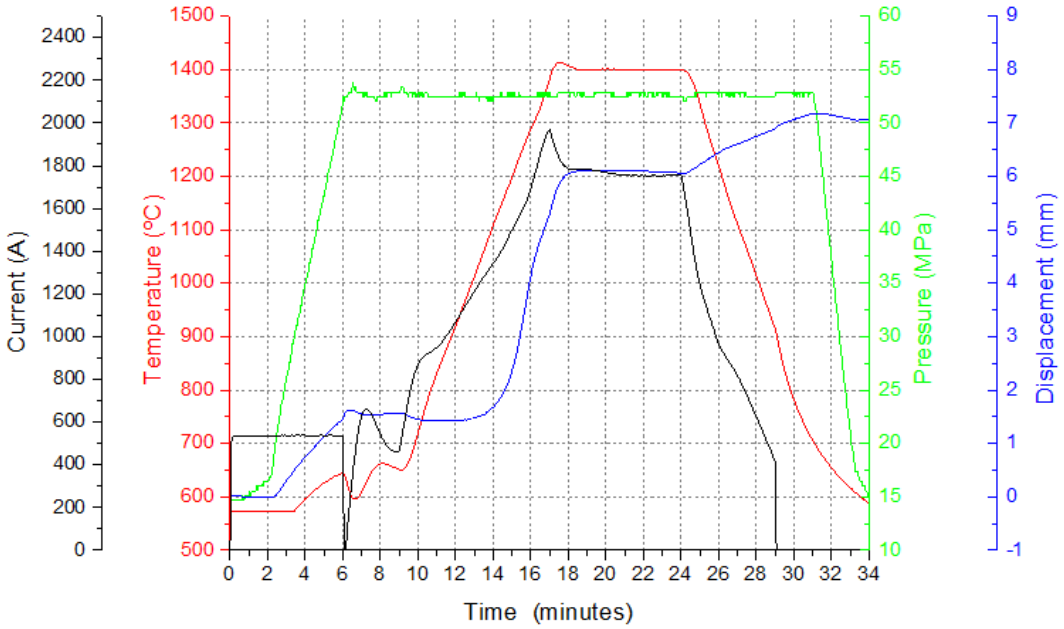

Figure 3. Monitoring of sintering variables current, temperature, pressure and displacement of sample with 5% ZrO_2.

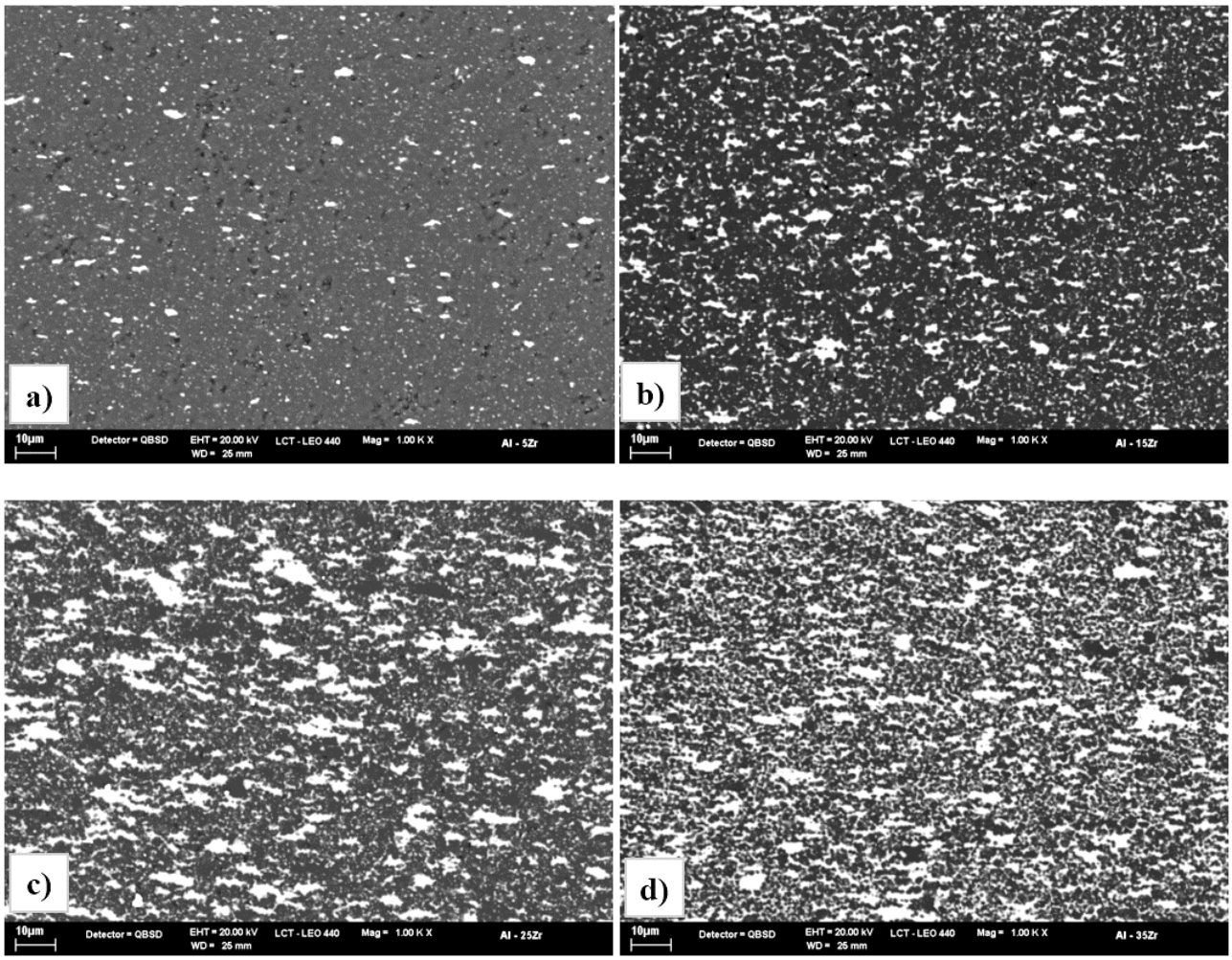

Figure 4. SEM images of alumina with (a) 5%, (b) 15%, (c) 25% and (d) 35% ZrO_2.

3.3 Relative density

Figure 5 shows the relative density results for the four volumetric ZrO_2 fractions. PECS sintering provides high density in a shorter sintering time when compared to conventional methods (Tokita, 1993). The porosity noticed in Figure 4 (a) is evidence that correlates with the mean relative density value for the 5% ZrO_2 sample. The results show an increase in the relative density with increasing ZrO_2 content, consequently decreasing the porosity percentage. The relative density for commercial ceramic was 98.2±0.3%. Then, considering mean density values, from the 15% ZrO_2 volume fraction, full densification can be regarded.

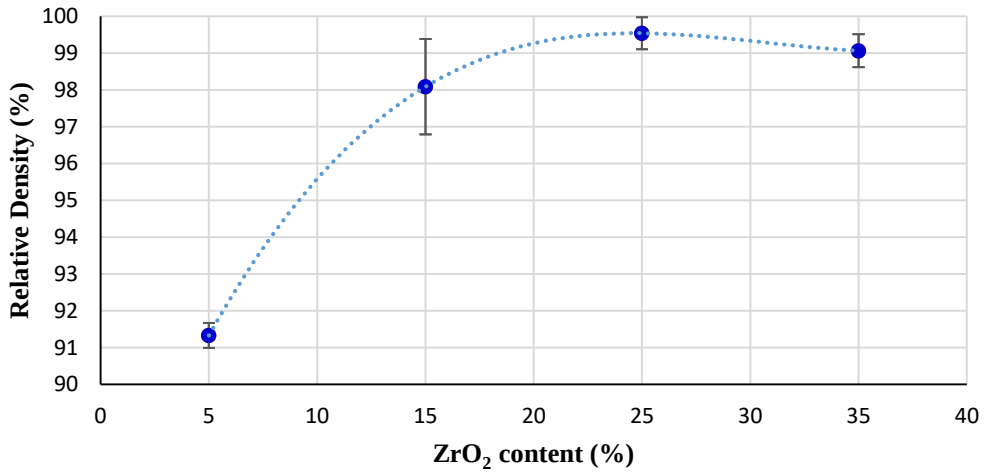

Figure 5. Relative density variation with increasing ZrO_2 content.

3.4 Hardness and fracture toughness (K_{IC})

Figure 6 shows the Vickers hardness curve as a function of ZrO_2 content. Using a literature reference value, red point, for monolithic alumina (Shen *et al.*, 2002), hardness decrease is verified by increasing the zirconia content. Kern *et al.* (2015) observed the same behavior with zirconia toughened alumina composites (ZTA). This fact can be related to the lower hardness of tetragonal zirconia in relation to alumina (Casellas *et al.*, 2003) and also the greater capacity to transform tetragonal zirconia into monoclinic phase, since hardness is inversely related to ease of transformation (Green *et al.*, 1989). Porosity of 8.67% for a sample with 5% ZrO_2 is another possible factor for the drop in hardness compared to monolithic alumina. However, despite the porosity, the Vickers hardness number evaluated for this sample (2007±35 HV) were higher than those tested, including the commercial ceramic (1712±306 HV).

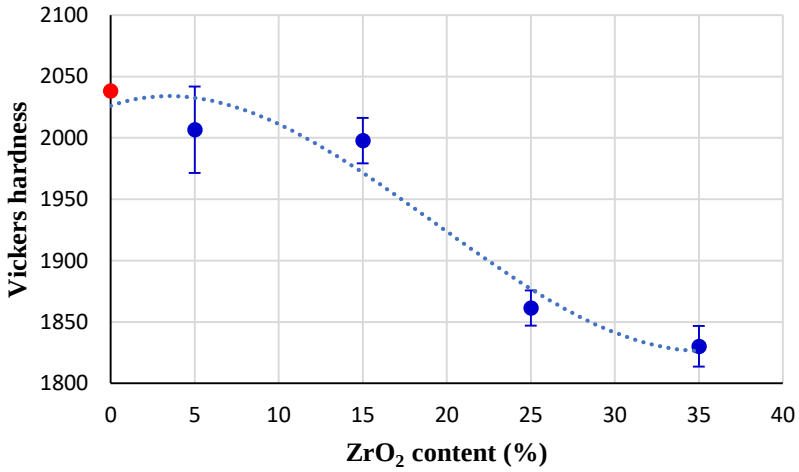

Figure 6. Vickers hardness for different ZrO_2 volume fractions.

In Figure 7, using a literature reference value of K_{IC} for monolithic alumina, black point (Shen *et al.*, 2002), the results showed that the addition of ZrO_2 in Al_2O_3 matrix promoted an increase in K_{IC} up to a threshold value, as mentioned by Trent and Wright (2000). After that, there was a drop in K_{IC} with additional ZrO_2 content. Using a reference value of K_{IC}

for monolithic alumina, a parabolic behaviour for the curve can be noted. The higher K_{IC} value obtained was 5.54±0.42 MPa.m$^{1/2}$ for 5% of ZrO_2 volume fraction. The commercial ceramic obtained 4.22±0.67 MPa.m$^{1/2}$. According to Smuk *et al.* (2003), the improvement in property is due to the phase transformation of ZrO_2 from tetragonal to monoclinic phase. This phase transformation is accompanied by an increase in volume, which induces compressive stresses around the crack tip, preventing its propagation, developing the toughening effect (Casellas *et al.*, 2003; Trent and Wright, 2000). However, for the 5% ZrO_2 sample, some porosity level might have been able to absorb fracture energy, changing the fracture mode and increasing the toughness (Kim *et al.*, 2016).

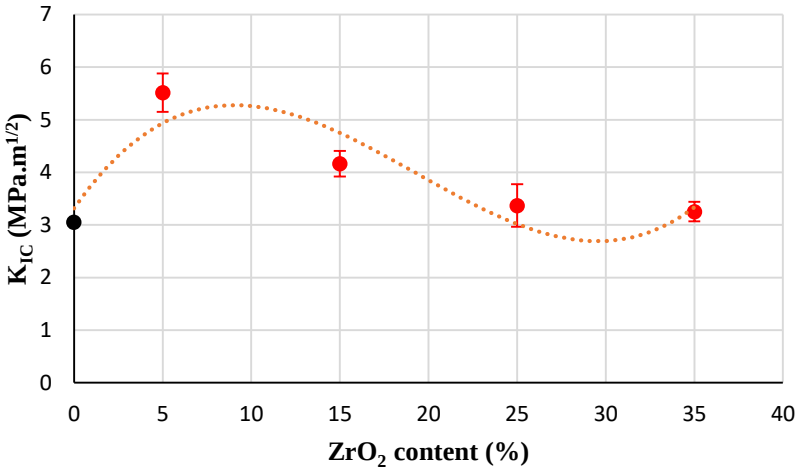

Figure 7. Fracture toughness for different ZrO_2 volume fractions.

Alumina-based ceramics are resistant to abrasion and hardness at high temperature, in addition to having chemical stability. Nevertheless, it has low fracture toughness. The addition of ZrO_2-$3Y_2O_3$ to the alumina matrix help to increase the fracture toughness. These results support further development towards a functionally graded ceramic.

4. CONCLUSION

Pulsed electric current sintering of four samples of α-alumina (ultrafine powder) with different ZrO_2-$3Y_2O_3$ (nanopowder) contents were investigated and the mechanical properties of the samples were defined. The PECS sintering technique, under the conditions of study, proved to be efficient for the thermal treatment of Al_2O_3-ZrO_2 composites. The results showed that the samples reached complete densification and, as expected, there was a decrease in the hardness value with the increase of the ZrO_2 content, while the fracture toughness value presented a parabolic behaviour, with elevation and then a decrease. Although the sample with 5% ZrO_2-$3Y_2O_3$ had about 8% porosity, it had a higher Vickers hardness number, 2007±35 HV, and K_{IC} 5.54±0.42 MPa.m$^{1/2}$. The results contribute to develop with optimized ZrO_2 content a functionally graded ceramic to be applied as a cutting tool.

5. ACKNOWLEDGMENT

The authors thank CAPES, FAPES (Grants 083/2019 and 144/2020) for providing research support.

6. REFERENCES

ASTM C1327-15, 2019, *American Society for Testing and Materials*. Standard Test Method for Vickers Indentation Hardness of Advanced Ceramics, ASTM International, 2019.

Basha, S.A.; Sarkar, D., 2020. "Grain growth suppression of ZTA by multi-step sintering". *Materials Today: Proceedings*, v. 26, p. 1226-1230.

Bertolete, M., Barbosa, P.A., Rossic, W., Fredericcid, C., Machado, I.F., 2020. "Mechanical characterization and machining evaluation of ceramic cutting tools functionally graded with six layers". *Ceramics International*, v.46, p. 15137-15145.

Boniecki, M., Gołębiewski, P., Wesołowski, W., Woluntarski, M., Piątkowska, A., Romaniec, M., Ciepielewski, P., Krzyżak, K., 2017. "Alumina/zirconia composites toughened by the addition of graphene flakes". *Ceramics International*, v.43, p. 10066-10070.

Casellas, D., Nagl, M.M., Llanes, L., Anglada, M., 2003. "Fracture toughness of alumina and ZTA ceramics: microstructural coarsening effects". *Journal of materials processing technology*, v. 143, p. 148-152.

German, R.M., 1996. *Sintering theory and practice*. New York: John Wiley & Sons Inc., 550 p.

German, R.M., 1998. ASM Handbook. Powder Metal Technologies and Applications. *ASM International*, v. 7, pp. 1020-1041.

German, R.M., Park, S.J., 2008. *Handbook of mathematical relations in particulate materials processing: ceramics, powder metals, cermets, carbides, hard materials, and minerals.* John Wiley & Sons.

Gong, F., Zhao, J., Li, Z., Sun, J., Ni, X., Hou, G., 2018. "Design, fabrication and mechanical properties of multidimensional graded ceramic tool materials". *Ceramics International*, v. 44, n. 3, p. 2941-2951.

Green, D.J., Hannink R.H.J., Swain M.V., 1989. *Transformation Toughening of Ceramics*, CRC Press, Boca Raton, FL.

ISO 10545-3, 2018, *International Organization for Standardization*. Ceramic tiles – Part 3: Determination of water absorption, apparent porosity, apparent relative density and bulk density, 2018.

Kalpakjian, S., Schmid, S., 2009. *Manufacturing Engineering and Technology*, SI Edition.

Kern, F., Palmero, P., Marro, F.G., Mestra, A., 2015. "Processing of alumina–zirconia composites by surface modification route with enhanced hardness and wear resistance". *Ceramics International*, v. 41, n. 1, p. 889-898.

Kim, Y.; Jo, H.; Allen, J.L.; Choe, H.; Wolfenstine, J.; Sakamoto, J. "The effect of relative density on the mechanical properties of hot-pressed cubic Li7La3Zr2O12". *Journal of the American Ceramic Society*, v. 99, p. 1367-1374. 2016.

Ma, J., Tan, G. E. B., 2001. "Processing and characterization of metal–ceramics functionally gradient materials". *Journal of Materials Processing Technology*, v. 113, n. 1-3, p. 446-449.

Mishina, H., Inumaru, Y., Kaitoku, K., 2008. "Fabrication of ZrO_2/AISI316L functionally graded materials for joint prostheses". *Materials Science and Engineering: A*, v. 475, n. 1-2, p. 141-147.

Miyamoto, Y., Kaysser, W. A., Rabin, B.H., Kawasaki, A., Ford, R.G., 1999. "Functionally graded materials: design, processing and applications". New York: *Springer*, 330 p.

Shen, Z., Johnsson, M., Zhao, Z., Nygren, M., 2002. "Spark plasma sintering of alumina". *Journal of the American Ceramic Society*, v. 85, n. 8, p. 1921-1927.

Smuk, B.; Szutkowska, M.; Walter, J., 2003. "Alumina ceramics with partially stabilized zirconia for cutting tools". *Journal of materials processing technology*, v. 133, n. 1-2, p. 195-198.

Tokita, M., 2000. "Mechanism of spark plasma sintering". In *Proceedings of 2000 Powder Metallurgy World Congress*, Kyoto, Japan, p. 729-732.

Tokita, M., 2013. "Spark plasma sintering (SPS) method, systems and applications". *Handbook of advanced ceramics*, p. 1149-1177.

Trent, E. M.; Wright, P. K., 2000. *Metal cutting*. Butterworth-Heinemann.

Watari, F., Yokoyama, A., Saso, F., Uo, M., Kawasaki, T., 1997. "Fabrication and properties of functionally graded dental implant". *Composites Part B: Engineering*, v. 28, n. 1-2, p. 5-11.

Xu, C., Xiao, G., Zhang, Y., Fang, B., 2014. "Finite element design and fabrication of Al2O3/TiC/CaF2 gradient self-lubricating ceramic tool material". *Ceramics International*, v. 40, n. 7, p. 10971- 10983.

Zhou, Y., Hirao, K., Yamauchi, Y., Kanzaki, S., 2004. "Densification and grain growth in pulse electric current sintering of alumina". *Journal of the European Ceramic Society*, v. 24, n. 12, p. 3465-3470.

7. RESPONSIBILITY NOTICE

The authors are the only responsible for the printed material included in this paper.